SYNTHESIS OF SUPERACID CATALYSTS $SO_4^{2-}/ZrO_2(Pt)$ AND $WO_x/ZrO_2(Pt)$ FOR ISOMERIZATION OF *n*-ALKANES

V.V. Brei[1], J. Fraissard[2], N.N. Levchuk[3], A.V. Melezhyk[1], and K.I. Patrylak[3]

[1]*Institute of Surface Chemistry, National Academy of Sciences, Kyiv, UKRAINE*
[2]*Laboratoire de Chimie des Surfaces, Universite Pierre et Marie Curie, Paris, FRANCE*
[3]*Institute of Bioorganic and Petroleum Chemistry, National Academy of Sciences, Kyiv, UKRAINE*

Abstract

Research has been conducted into the influence of the conditions of synthesis of SO_4^{2-}/ZrO_2 and WO_3/ZrO_2 systems and of doping of such systems with oxides of silicon and aluminium on their catalytic activity in *n*-hexane isomerization. An improved procedure for co-precipitation is used to synthezise superacid catalysts that exhibit high activity: the yield of branched isomers at 520 – 540 K is 65 – 70% with a selectivity for i-C_6 of 70 – 94% and *n*-hexane conversion of the order of 80%; the content of the most valuable substance, namely 2,2-dimethylbutane, in the isomerization products is 17 – 21 wt.%. $WO_x/ZrO_2(Pt)$ catalysts prove to be more stable than $SO_4^{2-}/ZrO_2(Pt)$. Doping of WO_3/ZrO_2 systems with oxides of aluminium, silicon, and niobium decreases their isomerization activity.

1. Introduction

Isomerization of linear alkanes C_5 – C_6, is employed for production of mixtures of branched isomers as high-octane additives to motor fuels. The process is effected in the presence of bifunctional acid catalysts based on the acidic form of mordenite [1] or chlorinated alumina [2] which contain platinum or palladium as dehydrogenating-hydrogenating components. Catalysts based on mordenite can function at a temperature of 520 – 570 K, which lowers the yield of branched isomers because of thermodynamic factors. Using chlorinated alumina makes it possible to carry out the process at relatively low temperatures (400 – 450 K) with high yields of isomers. However, this catalyst is rather sensitive to the presence of water and sulfur.

In recent years many research teams have conducted intensive studies of promising 'environmentally benign' catalysts for isomerization of *n*-alkanes based on sulfate and tungstate-containing zirconia which have superacid sites [3-19].

According to the agreed classification, superacids are compounds whose acid sites are characterized by Hammett function values that are lower than those for 100% sulfuric acid ($H_0 < -10$) [20]. Their number of solid superacids is not large and includes the synthetic polymer Nafion that contains $(CF_2)SO_3H$ groups ($H_0 \approx -12$); heteropolytungstates such as $Cs_{1.5}H_{0.5}PW_{12}O_{10}$ ($H_0 \approx -13$); $AlCl_3$-$CuCl_2$ and $AlCl_3$-$CuSO_4$ ($H_0 \approx -13.5$); sulfated oxides of titanium ($H_0 \approx -14.5$) and zirconium ($H_0 \approx -16$), and tungsten-containing zirconia WO_x/ZrO_2 ($H_0 \approx -14.5$) [3,4,20].

Among the familiar superacids, sulfated zirconia is outstanding in that it has the strongest acid sites and exhibits a high activity in the isomerization of paraffins [5,18]. However, it is known that SO_4^{2-}/ZrO_2 samples become deactivated due to loss of sulfur under the reductive conditions of the isomerization process. Nevertheless, catalysts based on sulfated zirconia doped with iron and manganese ions were tested in a pilot plant for *n*-butane isomerization [21]. Zirconia with a supported tungsten oxide phase WO_x/ZrO_2 is less acidic

than SO_4/ZrO_2 but it preserves its catalytic properties in reducing atmospheres at high temperatures. A few years ago Mobil Oil patented a number of catalysts based on WO_x/ZrO_2 which can be used for the isomerization of *n*-paraffins, the decyclization of cyclohexane, the hydrogenation of benzene, the alkylation of toluene with methanol, the oligomerization of olefins, the alkylation of C_6 aromatics with alkenes, the catalytic reduction of NO_x, as well as for the removal of sulfur and nitrogen compounds from crude oil [22].

There are detailed investigations on the methods of SO_4^{2-}/ZrO_2 and WO_x/ZrO_2 preparation which involve impregnation of zirconium hydroxide with solutions of sulfuric acid (or ammonium sulfate) and ammonium metatungstate (or co-precipitation of $ZrOCl_2$ and ammonium metatungstate using an aqueous solution of ammonia) followed by calcination of samples at 820 – 1170 K [6,9-11,13,14,16,17]. The activity of these catalysts is considerably dependent on the conditions of production of the starting zirconium hydroxide, of its sulfation or tungstation, drying, and calcination.

The objective of the present study was to compare the known procedures for synthesis of SO_4^{2-}/ZrO_2(Pt) and WO_x/ZrO_2(Pt) catalysts and to work out a method for the preparation of an active catalyst with reproducible properties for the isomerization of *n*-hexane. The study was also intended to consider the available data on the promoting effect of additives such as oxides of silicon, aluminium, and niobium on the catalyst activity in reactions of cumene cracking and *n*-hexane isomerization.

2. Experimental

2.1. *Catalysts Preparation*

Zirconium hydroxide samples were prepared by hydrolysis of chemically pure zirconyl chloride with an ammonia solution. 30 g of $ZrOCl_2 \cdot 8H_2O$ and 600 ml of H_2O were put into a round-bottomed flask equipped with a stirrer. Then, under conditions of continuous mixing at 320 - 330 K 15 ml of 13.5 *M* ammonia and 30 ml of water were added. In agreement with [6] the pH value of the zirconium hydroxide suspension formed was 8.0. The suspension was stirred at 320 K for 2 h, following which it was filtered using a Buchner funnel. The filtercake was washed with hot water (1 l) and dried at 370 K for 24 h.

Samples of the ZrO_2-SiO_2 system were prepared by grinding the zirconium hydroxide dried at 100 °C in a mortar with the addition of a small amount of water and, subsequently, 50 wt. % of Aerosil A-300. The paste obtained was pelletized to form cylindrical pellets 1 mm in diameter which were dried at 390 K for 2 h. Platinum and palladium were introduced by impregnating the samples with solutions of H_2PtCl_6 and $Pd(NO_3)_3$ to 0.5 wt. % of Pt(Pd), following which the samples were dried at 390 K for 2 h. Reduction of palladium ions was carried out in CO flow at 590 K, and reduction of Pt^{4+} - in hydrogen at the same temperature.

The samples were sulfated according to the following procedure. The dried samples were mixed with sulfuric acid solution, about 0.18 mol of H_2SO_4 per mole of ZrO_2. The acid concentration was adjusted so that the corresponding solution could be absorbed by the sample (3.3 ml of 2.33 *M* H_2SO_4 and 6 g of zirconium hydroxide; 8.4 ml of 0.5 *M* H_2SO_4 and 7 g of ZrO_2-SiO_2). The samples obtained were dried at 120 °C for 2 h. Finally the samples were calcined in air at 870 K for 2 h. Below this samples will be referred to as SO_4^{2-}/ZrO_2.

Samples of zirconium-tungstate catalysts (WO_x/ZrO_2) were prepared both by impregnation of zirconium hydroxide with an ammonium metatungstate solution and by co-precipitation from solutions of zirconyl chloride and ammonium metatungstate.

2.1.1. *Impregnation of zirconium hydroxide*. To a solution of zirconium oxychloride an ammonia solution was gradually added up to pH 9 - 10. The zirconium hydroxide precipitate formed was washed with water until no chloride ion was detected in the washing waters, following which it was dried at 370 K for 8 h and then at 410 K for 1.5 h. The product

obtained was impregnated with an ammonium metatungstate solution, dried, and calcined in a muffle furnace at 1070 K for 3 h. The WO_3 content in the calcined samples was 16-19 wt.%.

2.1.2. ***Samples* of WO_x/ZrO_2 *with addition of highly dispersed oxides of silicon and aluminium.*** The dried zirconium hydroxide prepared following procedure 2.1.1 was thoroughly ground in a mortar with highly dispersed pyrogenic alumina (140 $m^2\ g^{-1}$) and water [$(WO_3/ZrO_2):Al_2O_3$ = 4:1 w/w]. The paste formed was extruded, and the particles obtained were at first dried at 370 K and then at 410 K for 1.5 h, following which they were impregnated with an ammonium metatungstate solution, again dried at 370 K and calcined at 1070 K. In a similar way, samples with addition of Aerosil (300 $m^2\ g^{-1}$, $(WO_3/ZrO_2):SiO_2$ = =3:1 w/w) were synthesized.

2.1.3. ***Co-precipitation in aqueous solution.*** A solution of zirconium oxychloride in water containing ammonium metatungstate was refluxed simultaneously with slow introduction of ammonia by the "appearing reagent" method. In order to adjust the degree of hydrolysis the boiling time was varied from 1 to 13 h and the pH of the solution during the course of samples ageing from 1.0 to 7.9. The solutions obtained were then cooled and made alkaline by adding an ammonia solution up to pH 9.2 - 9.6, which led to gelation. The precipitates formed were thoroughly washed with water, following which these wet precipitates were extruded through a 2 mm diameter orifice. The particles obtained were dried in an oven and then heated in a muffle furnace at 1070 K for 3 h. The weight content of WO_3 in the synthesized catalysts amounted to 19 %, and their specific surface area was 40 – 55 $m^2\ g^{-1}$. This modified method gave four platinized samples with a gradually increasing degree of hydrolysis. Below they are denoted as WZrPt-1, WZrPt-2, WZrPt-3, and WZrPt-4.

Samples with addition of niobium oxide (WO_x/ZrO_2-Nb_2O_5) were synthesized according to the following procedure. To an initial solution of zirconium oxychloride was added a solution of niobium peroxide complex formed by interaction between precipitated niobium hydroxide and hydrogen peroxide in a nitric acid solution. The mixture was heated to decompose peroxide groups, and a solution of ammonium metatungstate added. The mixture was refluxed for 1 h, neutralized with ammonia up to pH 9, and then the resulting gel treated to obtain the calcined form as described above. The weight composition of the catalyst obtained was as follows: ZrO_2 = 74.8 %, WO_3 = 17.1 %, Nb_2O_3 = 8.1 %. Immediately before testing the WO_3/ZrO_2(Pt) catalysts in *n*-hexane isomerization they were reduced in a hydrogen flow at 620 – 670 K for 4 h.

2.2. *Methods for Characterizing the Catalysts*

X-ray diffraction patterns of samples were recorded on a DRON-UM1 diffractometer using Co Kα radiation. Specific surface area were measured by the standard method of low-temperature desorption of argon.

UV-Vis reflectance spectra of powdered samples were recorded on a Specord M-40 spectrophotometer. The relative reflection coefficient R was measured using MgO as a reference ($R = R_{sample}/R_{MgO}$). Absorption spectra of samples were calculated from their diffuse reflectance spectra with according to Kubelka-Munk function, $F(R) = (1-R)^2/2R$.

Acid characteristics were determined in terms of ammonia adsorption values at various temperatures of samples previously activated under vacuum as well as by the method of temperature-programmed desorption of ammonia using an MI-1201 mass spectrometer as analyser. The acidity of samples was also tested in cumene dealkylation, using the technique of temperature-programmed reaction (TPR) and mass-spectrometric monitoring of reaction products. Samples (4-8 mg) were put in a quartz cuvette and evacuated at 520 - 620 K (for mordenite, 720 K). Cumene adsorption was effected at 300 K. After evacuation the cuvette was hooked up to the bleed-in system of the MI-1201 mass spectrometer to register

concurrently the fragment ion $C_6H_5^+$ (77 a.m.u) and molecular benzene ion $C_6H_6^+$ (78 a.m.u.) with a linear increase of temperature (usually at a rate of 10 K min^{-1}).

The activity and selectivity of the catalysts were studied for *n*-hexane isomerization in a flow reactor. Samples in the form of pellets (0.5-1.0 mm in diameter) or worm-like particles (0.8 – 1.0 mm in diameter, 4 cm^3 in volume) were placed into an isothermal zone of the reactor and activated for 4 h at 670 K in a flow of hydrogen. Then the reactor was brought to stable operating conditions (pressure 3 MPa, temperature 500 – 540 K), following which it was fed with a mixture of hydrogen and *n*-hexane (H_2:*n*-C_6H_{14} = 1:1, LHVS =1 h^{-1}). Samples of products for analysis were taken at intervals of 1 h. The activity of the samples was stable throughout the 6- hour experiment. Products were analysed on a Khrom-4 gas chromatograph using a flame-ionization detector and capillary column 50 m long and 0.25 mm diameter with dinonyl phthalate as stationary phase.

3. Results and Discussion

3.1. *Sulfated Zirconia*

The X-ray diffraction patterns for the initial and sulfated zirconia are presented in Fig. 1. Calcination of an unsulfated sample at 870 K led to formation of the monoclinic modification of ZrO_2, with the specific surface area reduced from 230 to 40 m^2 g^{-1}. In the case of a sulfated sample the calcination treatment at the same temperature resulted in formation of a metastable predominantly tetragonal modification of ZrO_2, which is in agreement with [6,9]. Sulfate ions prevent sintering of a sample because its specific surface area decreased only to 100 m^2 g^{-1}. Introduction of highly dispersed silica increased the specific surface area of sulfated samples to 250 – 280 m^2 g^{-1}.

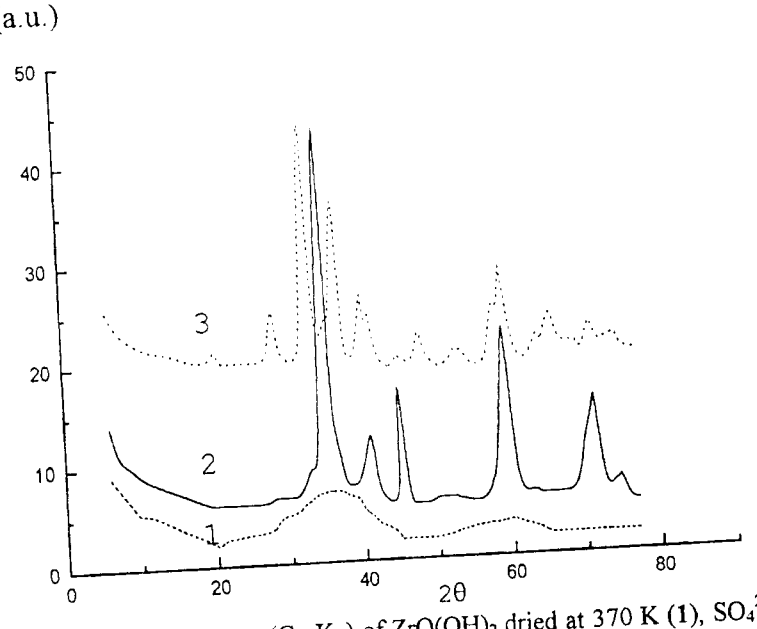

Fig. 1. X-ray diffraction patterns (Co K_α) of $ZrO(OH)_2$ dried at 370 K (**1**), SO_4^{2-}/ZrO_2 calcined at 870 K (**2**), and ZrO_2 calcined at 870 K (**3**).

B-sites (Bronsted sites) of sulfated zirconia were tested using Hammett indicators, and the results indicate that the absolute H_0 values are not smaller than 16 [3]. When in contact with a solution of 2,4-dinitrotoluene (pK_a = −13.75) the samples became yellow. These

samples exhibited high activity in cumene cracking which is one of the most important reactions for testing samples for their B-site strength.

In the TPR spectra recorded in the course of the formation of benzene from cumene adsorbed on SO_4^{2-}/ZrO_2 previously vacuum-treated at 520 K, the benzene peak was observed at 370 – 400 K (Fig. 2a). In the case of a less acidic H-mordenite the maximum of benzene release was observed at 440 – 460 K (Fig. 2b). The presence of platinum or palladium in the samples hardly affected the position of the maximum.

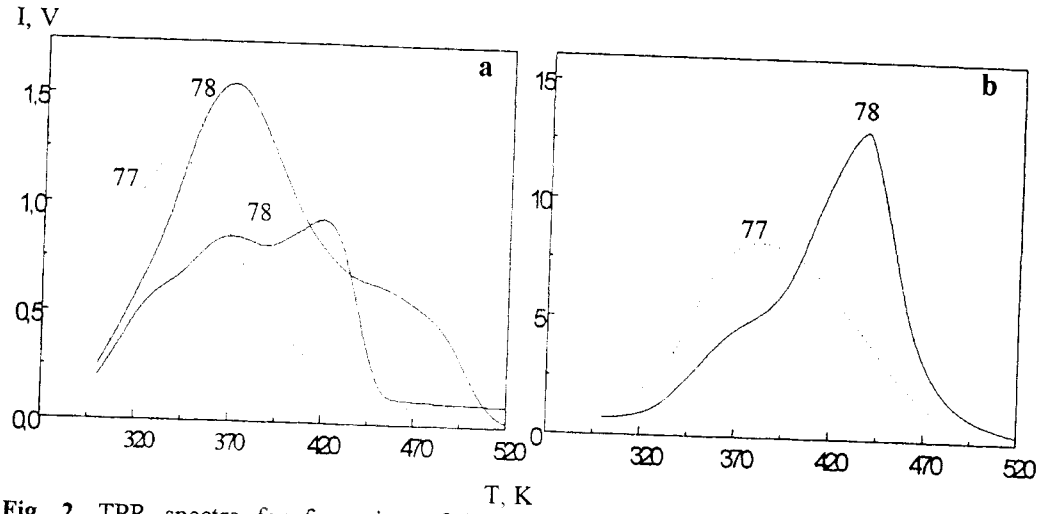

Fig. 2. TPR spectra for formation of benzene from cumene over SO_4^{2-}/ZrO_2 (**a**) and H-mordenite (**b**).
1- SO_4^{2-}/ZrO_2 freshly calcined at 870 K;
2- after exposing SO_4^{2-}/ZrO_2 one week in air.
Exceeding of the 78 a.u. mass curve over 77 a.u.m. indicates cracking of cumene.

Exposure of these samples to air led to a high-temperature shift of the benzene peak (T_m = 420 K) and to a decrease in its intensity (Fig. 2). After testing in *n*-hexane isomerization for 5 h the $SO_4^{2-}/ZrO_2(Pt)$ sample showed almost no activity in cumene cracking, with the sulfur content in the sample being decreased from 0.4 to 0.3 wt.%.

$SO_4^{2-}/ZrO_2(Pt)$ and SO_4^{2-}/ZrO_2-SiO_2(Pt, Pd) systems showed high activity in *n*-hexane isomerization (Table 1). The reaction products were predominantly 2-methylpentane, 3-methylpentane, 2,2-dimethylbutane with admixtures of cracking products (C_1 – C_5). The branched isomer yield at 500 K ranged from 62 to 75 % at a selectivity with respect to *i*-C_6 of 80 – 75 % and a *n*-hexane conversion of 78 – 83 %. For palladized H-mordenite similar results were achieved only at 530 – 550 K [1]. The above-mentioned data for $SO_4^{2-}/ZrO_2(Pt)$ at 500 K are very close to the data in [12]. Inclusion of highly dispersed silica into the composition of these catalysts led to a reduction in hexane cracking compared to $SO_4^{2-}/ZrO_2(Pt)$ at 500 – 520 K and to an increase (up to 17 %) in the yield of 2,2-dimethylbutane which is the most valuable product in terms of octane number. Comparison of the data on the yield and selectivity of branched isomers and the data on hexane cracking for SO_4^{2-}/ZrO_2-SiO_2(Pd) and SO_4^{2-}/ZrO_2-SiO_2(Pt) samples shows (see Table 1) that platinum is a more effective dehydrogenating-hydrogenating component of bifunctional catalysts for isomerization of *n*-alkanes than palladium, supposing that concentrations and strengths of active B-sites in the Pt- and Pd-containing catalysts are the same.

Table 1

Activity of catalysts on the basis of sulfated zirconium dioxide in the reaction of isomerization of *n*-hexane (volumetric flow rate of *n*-hexane: $1\ h^{-1}$, $P = 3.0$ MPa; H_2:$C_6H_{14} = 1:1$)

Catalyst	T, K	Composition of products according to chromatographic analysis data, wt.%										Conversion of *n*-hexane, %	Selectivity for Σi-C_6, wt.%
		$<C_4$	*i*-butane	*n*-butane	*i*-pentane	*n*-pentane	2,2-dimethyl-butane	2-methyl-pentane	3-methyl-pentane	ΣC_3-C_5	Σi-C_6	$>C_6$	*n*-hexane		
SO_4^{2-}/ZrO_2(Pt)	420	-	-	-	0.01	0.03	0.03	1.88	0.94	0.04	2.85	0.09	97.02	3.0	95.6
	470	0.01	0.03	0.03	0.04	0.04	0.67	12.71	6.88	0.15	20.26	0.05	79.54	20.5	98.8
	500	0.46	3.89	0.62	5.33	1.93	15.73	36.84	17.77	12.23	70.34	0.13	17.30	82.7	85.1
	520	The liquid phase yield sharply decreased, the gas phase contained predominantly propane and *i*-butane (1:1).													
SO_4^{2-}/ZrO_2-SiO_2(Pt)	420	-	-	-	0.22	-	0.18	1.99	1.02	0.22	3.19	0.09	96.50	3.5	91.1
	470	0.00	0.14	0.07	0.02	0.04	0.18	6.72	3.56	0.27	10.46	0.11	89.16	10.8	96.9
	500	0.10	0.37	0.14	0.47	0.13	11.00	42.15	22.93	1.21	76.08	0.09	22.62	77.4	98.3
	520	0.12	0.46	0.34	3.17	1.74	17.26	37.88	20.26	5.83	75.40	0.00	18.77	81.2	92.3
SO_4^{2-}/ZrO_2-SiO_2(Pd)	420	0.00	0.01	0.00	0.03	0.06	0.14	2.54	1.27	0.10	3.95	0.16	95.79	4.2	94.0
	470	-	0.01	0.00	0.06	0.03	0.56	12.50	6.63	0.10	19.69	0.10	80.11	19.9	98.9
	500	0.46	4.86	0.75	6.17	1.31	7.79	37.10	17.47	13.55	62.36	2.16	21.93	78.1	79.8
	520	0.97	9.19	2.26	14.96	5.29	11.29	28.12	13.19	32.67	52.60	1.05	13.68	86.3	61.0

3.2. *Tungsten-containing Zirconia*

As is seen from the diffraction patterns (Fig. 3), after calcination at 1070 K zirconium hydroxide without addition of W or Nb is almost purely monoclinic ZrO_2 phase (the most intense peaks at 2Θ = 32.9° and 36.8°). Addition of WO_3 leads to formation of a predominantly tetragonal phase of ZrO_2 (the most intense peak at 2Θ = 35.3°). This observation agrees with the known data [13] according to which the addition of tungstate groups stabilizes the tetragonal zirconia phase that otherwise is metastable at these temperatures. Of note also is the fact that the decrease in the specific surface area of samples observed during the course of their thermal treatment is substantially smaller than that for zirconium hydroxide without such additives. On the diffraction patterns for Nb-containing samples there are no peaks that could be attributed to a monoclinic phase. Niobium pentoxide seems to stabilize the tetragonal phase of ZrO_2 more efficiently than WO_3 does.

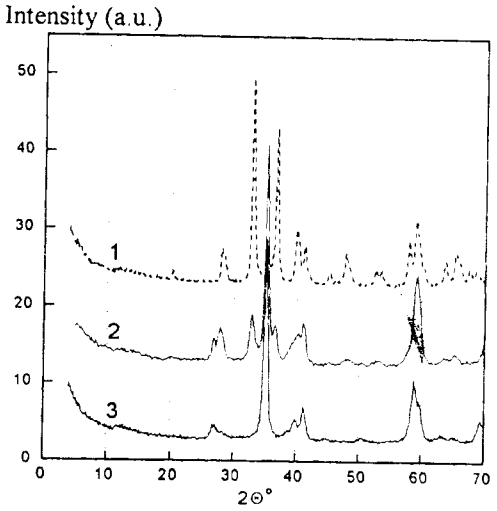

Fig.3.
X-ray diffraction patterns (CoK_α) of ZrO_2 (1), WO_3/ZrO_2 (2), and WO_3-Nb_2O_5/ZrO_2 (3).

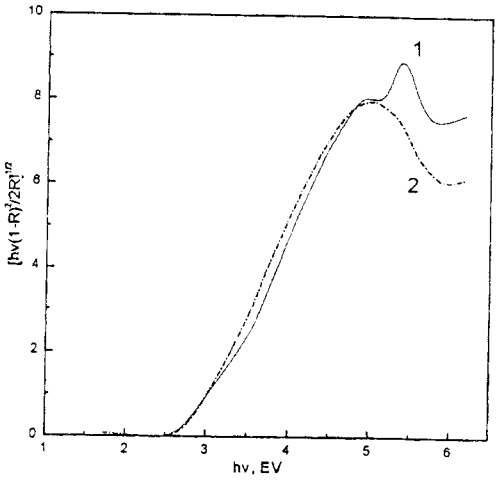

Fig. 4.
UV-Vis reflectance spectra for WO_3/ZrO_2 (1) and WO_3-Nb_2O_5/ZrO_2 (2).

The $[hv(1-R)^2/2R]^{1/2}$ function for WO_3/ZrO_2 samples calculated from their diffuse reflectance spectra are shown in Fig. 4. In the case of semiconductors oxides this function is approximately linear on the long-wavelength edge of the absorption band, and the intercept of the extrapolated linear portion of such a dependence makes it possible to determine forbidden gap values. For WO_3 clusters the forbidden gap decreases with increasing cluster size [19]. According to [19] for the WO_3/ZrO_2(Pt) system the highest catalytic activity in reactions catalysed by superacidic sites is observed in the case of samples with a certain optimum size of WO_3 clusters whose E_0 values are approximately 3.1 – 3.2 eV. The $[hv(1-R)^2/2R]^{1/2}$ vs. hv plots for our samples are similar to those presented in [19]. The inflection points in the long-wavelength region give evidence for the presence of WO_3 crystallites.

The weak peaks in the 2Θ interval from 27.0 to 28.4° in the diffraction patterns (Fig. 3) may be assigned to a monoclinic WO_3 phase (E_0 = 2.64 eV [19]) whose most intense peaks are at 2Θ =27.0, 27.5, 28.4, and 39.9° (recalculated for Co Kα radiation). Thus, high-temperature treatment of samples causes the initially homogeneous hydroxide structure of the samples to be divided into ZrO_2 and WO_3 phases.

Gravimetric curves of ammonia thermal desorption from the surface of samples allow one to estimate the concentration of acid sites (Fig. 5). Reduction of the WO_x/ZrO_2 sample promoted with platinum in a flow of hydrogen at 670 K for 4 h leads to a small increase in the content of strongly retained ammonia that undergoes desorption at temperatures above 420 K. This concentration makes up 0.16 mmol g^{-1} in comparison with 0.12 mmol g^{-1} for an unreduced WO_3/ZrO_2 sample. The concentration of acid sites determined for both samples by back- titration of *n*-butylamine adsorbed from toluene solutions is 0.13 mmol g^{-1}. If *tert*-butylamine is used, the acid site concentrations obtained for all the samples are approximately 20 % smaller than those determined with *n*-butylamine. This fact is related to the different accesibilities of acid sites to molecules of ammonia, *n*-butylamine, and *tert*-butylamine.

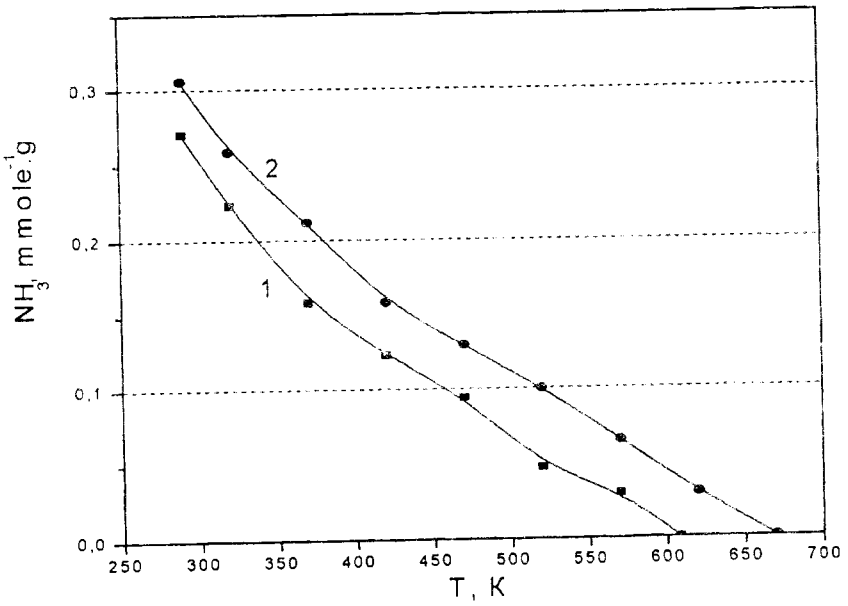

Fig. 5. Gravimetric curves for thermal desorption of ammonia for WO_3/ZrO_2 **(1)** and WO_x/ZrO_2(Pt) **(2)**.

In the case of a reduced WO_x/ZrO_2(Pt) sample the content of sites that are more acidic than in H-mordenite (desorption of ammonia at temperatures above 600 K) is 0.035 mmol g^{-1} (Fig. 5). Evaluation of the acidity of tungstate-containing ZrO_2 using Hammett indicators is impossible because after calcination at 1070 K the samples become yellow and after reduction they become black-blue. We have evaluated the concentration of acid sites in terms of 4-nitrotoluene (4-NT) adsorption ($pK_a = -11.38$) from toluene solutions. The concentration of 4-NT was determined photometrically. The amount of 4-NT adsorbed on the WO_3/ZrO_2 sample is 0.028 mmol g^{-1} whereas that adsorbed on the WO_x/ZrO_2(Pt) sample is equal to only 0.004 mmol g^{-1}. The last value is close to the content of acid sites (that are active in isomerization of *n*-pentane) which was calculated on the basis of poisoning of the WO_x/ZrO_2 catalyst by 2,6-dimethylpyridine [14]. It may be assumed that the enhanced adsorption of 4-NT on the WO_3/ZrO_2 sample is due to formation of charge-transfer surface complexes.

As distinct from the SO_4^{2-}/ZrO_2 samples, the WO_x/ZrO_2 catalysts preserve their activity after long-term storage in air. As far as cumene cracking is concerned, reduced samples of WO_x/ZrO_2 are more efficient than WO_3/ZrO_2 (Fig. 6). The highest activity is exhibited by the tungstate-containing ZrO_2 promoted with Nb_2O_5. Addition of highly dispersed alumina leads to a

decrease in the catalytic activity. However, it should be noted that there is no direct correlation between the WO_x/ZrO_2 sample activity in the reactions of cumene cracking and *n*-hexane isomerization as there was for SO_4^{2-}/ZrO_2.

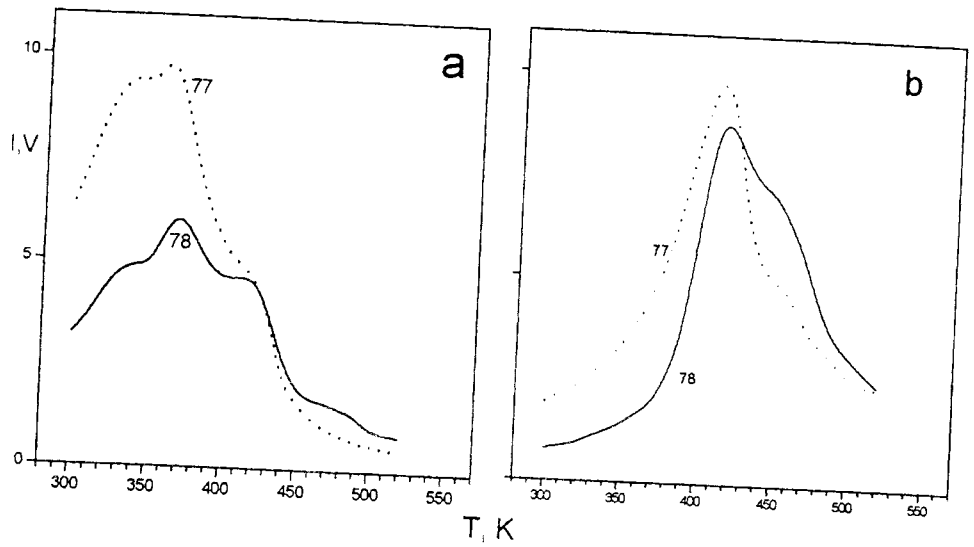

Fig. 6. TPR spectra for formation of benzene from cumene over WO_3/ZrO_2 (**a**) and WO_x/ZrO_2(Pt) (**b**). Exceeding of the 78 a.u. mass curve over 77 a.u.m. indicates cracking of cumene.

We synthesized samples of WO_x/ZrO_2 following the usual procedures [22]. When they are tested in *n*-hexane isomerization, the published results are difficult to reproduce. Thus, for catalysts prepared by the impregnation method the *n*-hexane conversion was 4 % at 470 K and 14 % at 520 K. These values are smaller than those cited in the corresponding patents [22]. The results achieved by the co-precipitation method for obtaining WO_3/ZrO_2 are more reproducible. With a view to synthesizing active zirconium-tungstate catalysts we modified the accepted method for co-precipitating hydroxides of zirconium and tungsten as described above (section 2.1.3). The WZrPt samples prepared following the above-described modified co-precipitation procedure exhibit high activity in *n*-hexane isomerization (Table 2). As for the SO_4^{2-}/ZrO_2(Pt) catalysts, the reaction products are predominantly 2-methyl pentane, 3-methylpentane, and 2,2-dimethylbutane with admixtures of cracking (C_1 – C_5) and condensation (C_{6+}) products. If WZrPt-3 and WZrPt-4 samples were preliminarily activated in a hydrogen flow, at 520-540 K the branched isomer yield is 65 – 70%, with a selectivity for i-C_6 of 70 – 94% and *n*-hexane conversion of the order of 80%. These results are close to the corresponding patent information [22]. It should also be noted that the WZrPt catalysts allow one to attain higher contents of the most valuable product, namely 2,2-methylbutane (2,2-DMB/Σi-C_6 is 17 to 21wt%).

When the catalyst composition includes highly dispersed silica and, especially, highly dispersed alumina, the yield of *n*-hexane isomers decreases sharply. In this case the main product is benzene with admixtures of other aromatic hydrocarbons, which indicates that the WO_x/ZrO_2-$Al_2O_3(SiO_2)$(Pt) systems predominantly catalyse the dehydrocyclization of *n*-hexane. Addition of niobium leads to a decrease in *n*-hexane conversion and 2,2-dimethylbutane yield but the selectivity for i-C_6 remains high.

Table 2

Activity and selectivity of catalysts on the basis of tungstate-containing zirconia in the reaction of isomerization of *n*-hexane (volumetric flow rate of *n*-hexane: 1 h^{-1}; P = 3.0 MPa; H_2:C_6H_{14} = 1:1; Pt content = 0.5 wt.%)

Catalyst	T, K	Conversion of *n*-hexane, %	Selectivity for Σi-C_6, wt.%	Content of 2,2-DMB in Σi-C_6, wt.%	Composition of reaction products, wt.%								
					propane	*i*-butane	*n*-butane	*i*-pentane	*n*-pentane	2,2-dimethyl-butane (DMB)	2-methylpentane	3-methylpentane	>C_6
WZrPt-1	500	72.7	97.4	12.9	0	0.1	0.1	0.6	0.2	9.1	37.7	23.9	0.9
	540	81.9	67.8	21.1	0.6	4.2	2.3	11.9	6.2	11.7	26.4	17.4	1.1
WZrPt-2	520	77.5	93.1	19.6	0	1.0	0.2	2.6	1.2	14.1	36.9	21.2	0.4
	540	81.0	73.1	16.6	0.9	6.4	2.2	7.9	3.5	9.8	30.1	19.3	1.0
WZrPt-3 without reduction	500	58.2	98.2	4.1	0	0	0	0.2	0.2	2.4	35.5	19.3	0.6
	520	66.7	97.9	5.3	0	0	0	0.1	0.1	3.4	38.8	23.0	1.2
	540	71.4	98.5	15.6	0	0	0	0.2	0.2	10.9	37.5	21.9	0.7
WZrPt-3	520	81.1	93.8	21.5	0	0.4	0.2	2.7	1.0	16.3	39.0	20.8	0.6
	540	78.8	87.9	16.0	0	0.9	0.5	5.2	2.2	10.9	36.1	21.3	0.6
WZrPt-4	500	79.8	96.3	18.7	0	0.2	0.1	1.2	0.5	14.4	40.6	21.9	0.7
	520	80.8	88.4	16.8	0.5	2.2	0.8	3.7	1.4	12.0	39.0	20.5	0.8
	540	86.8	69.0	20.3	0.6	6.1	3.0	12.4	4.4	12.1	29.7	18.1	0.4
WO_xZrO_2 without Pt	500	50.4	88.4	7.4	0.1	1.4	0.3	2.6	0.6	3.3	27.4	13.8	0.9
	520	47.9	87.2	6.5	0.2	1.6	0.3	2.8	0.3	2.7	24.8	14.3	0.9
	540	54.8	89.4	5.1	0.2	1.4	0.3	2.6	0.5	2.5	30.2	16.3	0.8
WO_x/ZrO_2-Nb_2O_5(Pt)	500	41.9	97.1	3.4	0	0	0	0	0.1	1.4	25.9	13.4	1.1
	540	65.1	96.0	11.3	0.1	0.3	0.3	0.9	0.3	7.1	36.6	18.8	0.8

It is assumed that superacid sites in the form of H-tungstate bronze clusters $(WO_3)_m(W^{6-n}O_3)(n\ H^+)$ appear during reduction of the WO_3 phase with hydrogen on the ZrO_2 surface [19]. Of note is the fact that catalytic activity is exhibited only by clusters of certain sizes, namely by clusters whose formation requires treatment of samples of mixed oxides of zirconium and tungsten at 970 – 1170 K. The tungstate bronzes are known to have high electronic conductivity. The tetragonal phase of ZrO_2 accepts electrons of WO_x clusters, which weakens the Coulombic attraction between protons and clusters, and enhances the acid strength of B sites. It may be suggested that conductive clusters of H-tungstate bronzes could effect dehydrogenation-hydrogenation of alkanes, i.e. could behave similarly to platinum and palladium. However, our experimental results show (Table 2) that exclusion of platinum from the catalyst composition leads to a considerable decrease in *n*-hexane conversion.

Several mechanisms for *n*-alkane isomerization on bifunctional heterogeneous catalysts are discussed in the literature. The most frequently cited mechanism involves dehydrogenation of a paraffin to olefin as an intermediate and absorption of hydrogen by platinum or palladium, protonation of the olefin through the use of B sites of the catalyst, isomerization proper of carbenium ions and hydrogenation of the isoolefin to isoparaffin [6]. The negative order of the isomerization reaction with respect to hydrogen gives strong evidence for this mechanism [7].

In another mechanism for *n*-alkane isomerization, it is suggested that the process includes following stages: 1) protonation of alkane molecules by the strongly acidic B-sites, 2) formation of a carbonium ion with a 5-coordinated carbon atom, 3) abstraction of two hydrogen atoms from this ion with the participation of platinum, 4) isomerization of the carbonium ion through the transient cyclopropane state, and 5) addition of a hydride ion to the isomer and that of a proton to the deprotonated B-site [5]. The transport of hydride ions to isomeric carbonium ions is assumed to be a rate-determining step of the isomerization process [5]. It is evident that this mechanism does not involve formation of an olefin.

According to [23, 24], isomerization of *n*-alkanes on sulfated zirconia proceeds with participation of strong Lewis sites (zirconium ions) which abstract hydride ions from hydrocarbon molecules. The carbenium ions formed are synchronously attached to bridging hydrogen atoms and, as a consequence, undergo isomerization. In the final stage the sites are regenerated with desorption of isoparaffin molecules.

Thus, it is evident that to establish the true mechanism of *n*-alkanes isomerization on bifunctional acid catalysts additional experimental data are required.

4. Conclusion

The $SO_4^{2-}/ZrO_2(Pt)$ and $WO_x/ZrO_2(Pt)$ catalysts synthesized exhibit high activity in *n*-hexane isomerization at 520 – 540 K (*n*-hexane conversion: 80–85%, isomers yield 65 – 70%, selectivity for *i*-C_6: 70 – 94%). $WO_x/ZrO_2(Pt)$ catalysts prove to be the more stable. The comparative study of impregnation and co-precipitation methods for producing tungstate-containing zirconia shows that catalysts co-precipitated following an improved procedure are more active in *n*-hexane isomerization. Promotion of SO_4^{2-}/ZrO_2 systems with highly dispersed silica leads to an increase in their specific surface area without loss of catalytic activity, whereas promotion of WO_3/ZrO_2 systems with highly dispersed oxides of silicon and aluminium is accompanied by a decrease in catalytic activity.

References

1. Patrylak K.I., Bobonych F.M., Voloshyna Yu.G., Levchuk M.M., Il'in V.G., Yakovenko O.M., Manza I.A., Tsupryk I.M. Ukrainian mordenite-clinoptilolite rocks as a base for linear hexane isomerization catalyst //Appl. Catal. A. - 1998. - V. 174. - P. 187-198.

2. Mangnus P.J., Jacobs A. - in B. van Keulen (Ed.), Akzo Catalysts Symposium. Hydroprocessing, Akzo Chem. Div., Amersfort, Netherlands. - 1991. - P. 163.
3. Hino M., Arata K. Synthesis of Solid Superacid Catalyst with Acid Strength of $H_o \leq -16.04$ //J. Chem Soc., Chem. Commun. - 1980. - N. 18. - P. 851-852.
4. Hino M., Arata K. Synthesis of Solid Superacid of Tungsten Oxide Supported on Zirconia and its Catalytic Action for Reactions of Butene and Pentane //J. Chem Soc., Chem. Commun. - 1988. - N. 18.- P. 1259-1260.
5. Iglesia E., Soled S.L., Kramer G.M. //J. Catal. - 1993-V. 144. - P. 238.
6. Tatsumi T., Matsuhashi H., Arata K. A Study of the Preparation Procedure of Sulfated Zirconia Prepared from Zirconia Gel. The Effect of the pH of the Mother Solution on the Isomerization Activity of n-Pentane //Bull. Chem. Soc Japan. - 1996. - V. 69. - N. 5. - P. 1191-1194.
7. Avdeeva V., de Haan J.W., Janchen J., Lei G.D., Schunemann V., van de Ven L.J.M., Sachtler W.M.H., van Santen R.A. Acid Sites in Sulfated and Metal-Promoted Zirconium Dioxide Catalysts //J. Catal. - 1995. - V. 151. - P. 364-372
8. Morterra C., Cerrato G., Pinna F., Signoretto M., Strukul G. On the Acid-Catalyzed Isomerization of Light Parraffins over a ZrO_2/SO_4 System: The Effect of Hydration //J. Catal. - 1994.- V. 149. - N 1. - P. 181-188.
9. Ward D.A., Ko E.I. One-Step Synthesis and Characterization of Zirconia-Sulfate Aerogels as Solid Superacids //J. Catal. - 1994. - V. 150. - N 1. - P. 18-33.
10. Lopez T., Navarrete J., Gomez R., Novaro O., Figueras F., Armendariz H. Preparation of Sol-Gel Sulfated ZrO_2-SiO_2 and Characterization of its Surface Acidity //Appl. Catal. A - 1995. - V. 125. N. 2. - P. 217-232.
11. Navio J.A., Colon G., Masfas M., Campelo J.M., Romero A.A., Marinas J.M. Catalytic Properties of ZrO_2-SiO_2: Effects of Sulfation in the Cyclohexene Isomerization Reaction //J. Catal. - 1996. - V. 161. - P. 605-613.
12. Gonzalez M.R., Kobe J.M., Fogash K.B., Dumesic J.A. Promotion of n-Butane Isomerization Activity by Hydration of Sulfated Zirconia //J. Catal. - 1996. - V. 160. - P. 290-298.
13. Boyse R.A., Ko E.I. Crystallization Behaviour of Tungstate on Zirconia and its Relationship to Acidic Properties. I. Effect of Preparation Parameters //J. Catal. -1997. - V. 171. - N. 1. - P. 191- 207.
14. Santiesteban J.G., Vartuli J.C., Han S., Bastian R.D., Chang C.D. Influence of the Preparative Method on the Activity of Highly Acidic WO_x/ZrO_2 and the Relative Acidity Compared with Zeolites //J. Catal. - 1997. - V. 168. - P. 431-441.
15. Iglesia E., Barton D.G., Biscardi J.A., Gines M.J.L., Soled S.L. Bifunctional pathways in catalysis by solid acids and bases //Catalysis Today. - 1997. --V. 38 - N 3. - P. 339-360.
16. Barton D.G., Soled S.L., Iglesia E. Solid Acid Catalysts Based on Supported Tungsten Oxides //Topics in Catalysis. - 1998. V. 6 - P. 87-99.
17. Scheithauer M., Cheung T.-K., Jentoff R.E., Grasselli R.K., Gates B.C., Knözinger H. Characterization of WO_x/ZrO_2 by Vibrational Spectroscopy and n-Pentane Isomerization Catalysis //J. Catal. - 1998. - V. 180. N 1. - P. 1-13.
18. Ivanov A.V., Vasina T.V., Masloboishchikova O.V., Khelkovskaya-Sergeeva E.G., Kustov L.M., Zoiten P. Investigation of Alkane Isomerization in Presence of Superacid Catalysts Based on SO_4/ZrO_2 //Kinetika i Kataliz. - 1998. - V. 39 N. 3. - P. 396-406.
19. Barton D.G., Shtein M., Wilson R.D., Soled S.L., Iglesia E. Structure and Electronic Properties of Solid Acids Based on Tungsten Oxide //J. Phys. Chem. B. - 1999. - V. 103 - P. 630-640.
20. Corma A. Inorganic Solid Acids and their Use in Acid-Catalyzed Hydrocarbon Reactions //Chem. Rev. - 1995. - V. 95. - N 3. - P. - 559-614.

21. Tanabe K., Holderich W.F. Industrial Application of Solid Acid-Base Catalysts //Appl. Catal. A. - 1999. V. 181. - P. 399-434.
22. Mobil Oil Corp., US Patents 5,345,026 (1994); 5,382,731 (1995); 5,449,847 (1995); 5,516,954 (1996); 5,563,310 (1996); 5,608,133 (1997).
23. Tanabe K. Catalysts and catalytic processes. - Moscow: Mir, 1993. (In Russian).
24. Dushet J., Guillaume D., Monnier A., van Gestel J., Szabo G., Nascimento P., Decker S. //J. Chem.Soc., Chem. Commun. - 1999. - P. 1819.